L-Methionine Sulfoximine, but Not Phosphinothricin, Is a Substrate for an Acetyltransferase (Gene PA4866) from *Pseudomonas aeruginosa*: Structural and Functional Studies

Anna M. Davies,‡ Renée Tata,‡ Rebecca L. Beavil, Brian J. Sutton, and Paul R. Brown*,‡

Randall Division of Cell and Molecular Biophysics, King's College London, New Hunt's House, Guy's Campus, London Bridge, SE1 1UL, London, U.K.

Received July 28, 2006; Revised Manuscript Received November 22, 2006

ABSTRACT: The gene PA4866 from *Pseudomonas aeruginosa* is documented in the *Pseudomonas* genome database as encoding a 172 amino acid hypothetical acetyltransferase. We and others have described the 3D structure of this protein (termed pita) [Davies et al. (2005) *Proteins: Struct., Funct., Bioinf. 61*, 677−679; Nocek et al., unpublished results], and structures have also been reported for homologues from *Agrobacterium tumefaciens* (Rajashankar et al., unpublished results) and *Bacillus subtilis* [Badger et al. (2005) *Proteins: Struct., Funct., Bioinf. 60*, 787−796]. Pita homologues are found in a large number of bacterial genomes, and while the majority of these have been assigned putative phosphinothricin acetyltransferase activity, their true function is unknown. In this paper we report that pita has no activity toward phosphinothricin. Instead, we demonstrate that pita acts as an acetyltransferase using the glutamate analogues L-methionine sulfoximine and L-methionine sulfone as substrates, with $K_{m(app)}$ values of 1.3 ± 0.21 and 1.3 ± 0.13 mM and $k_{cat(app)}$ values of 505 ± 43 and 610 ± 23 s^{-1} for L-methionine sulfoximine and L-methionine sulfone, respectively. A high-resolution (1.55 Å) crystal structure of pita in complex with one of these substrates (L-methionine sulfoximine) has been solved, revealing the mode of its interaction with the enzyme. Comparison with the apoenzyme structure has also revealed how certain active site residues undergo a conformational change upon substrate binding. To investigate the role of pita in *P. aeruginosa*, a mutant strain, Depp4, in which pita was inactivated through an in-frame deletion, was constructed by allelic exchange. Growth of strain Depp4 in the absence of glutamine was inhibited by L-methionine sulfoximine, suggesting a role for pita in protecting glutamine synthetase from inhibition.

In most organisms the *ureA*, *ureB*, and *ureC* genes that encode the three subunits of urease are contiguous (*3*), but in *Pseudomonas aeruginosa* a gene, PA4866 (*pita*), is situated between the *ureA* and *ureB* genes (http://www.pseudomonas.com). PA4866 encodes a 172 amino acid protein (pita) that is designated as a hypothetical acetyltransferase belonging to the GNAT (GCN5-related *N*-acetyltransferase) family (PF00583; *4*, *5*), and we have shown that the 3D structure of pita from *P. aeruginosa* strain PAC1 has features common to this family (*1*). Recently, structures have also been solved for pita from *P. aeruginosa* strain PAO1 (PDB code 1YVO; Nocek et al., unpublished results) and pita-like enzymes from *Agrobacterium tumefaciens* (PDB code 1YR0; Rajashankar et al., unpublished results) and *Bacillus subtilis* [PDB code 1VHS (*2*)], revealing a similar protein fold.

Blast searches have revealed that pita-like enzymes are widely distributed among Gram-negative and Gram-positive bacteria (Figure 1). The majority of these enzymes have been assigned putative phosphinothricin *N*-acetyltransferase activity on the basis of sequence similarities with the phosphinothricin acetyltransferases synthesized by *Streptomyces viridochromogenes* (*8*) and *Streptomyces hygroscopicus* (*9*). Demethylphosphinothricin is an intermediate in the biochemical pathway leading to the formation of Bialaphos. Bialaphos is a highly efficient herbicide that is hydrolyzed in the soil releasing phosphinothricin, a glutamate analogue (Figure 2), that inhibits glutamine synthetase (GS),[1] causing plant death, apparently through the resulting accumulation of ammonium. Protection for crops against the action of phosphinothricin has been achieved by genetic modification of the plants to incorporate the *bar* gene that expresses phosphinothricin acetyltransferase (*10*). Pita has 34.8% and 36.7% sequence identity with the phosphinothricin acetyltransferases from *S. viridochromogenes* and *S. hygroscopicus*, respectively.

While the majority of pita-like enzymes have been assigned putative phosphinothricin acetyltransferase activity, their true function has not yet been determined. The results reported in this work show that pita cannot be classified as a phosphinothricin acetyltransferase. We demonstrate that pita is able to utilize the glutamate analogues L-methionine sulfoximine (L-metsox)[1] and L-methionine sulfone (L-metsone)[1] (Figure 2) as substrates but displays no activity toward phosphinothricin. We have solved a high-resolution (1.55

* To whom correspondence should be addressed. Phone: +44 (0) 20 7848 6560. Fax: +44 (0) 20 7848 6410. E-mail: paul.brown@kcl.ac.uk.
‡ These authors contributed equally to this work.

[1] Abbreviations: L-metsox, L-methionine sulfoximine; L-metsone, L-methionine sulfone; GS, glutamine synthetase.

10.1021/bi0615238 CCC: $37.00
Published on Web 01/25/2007

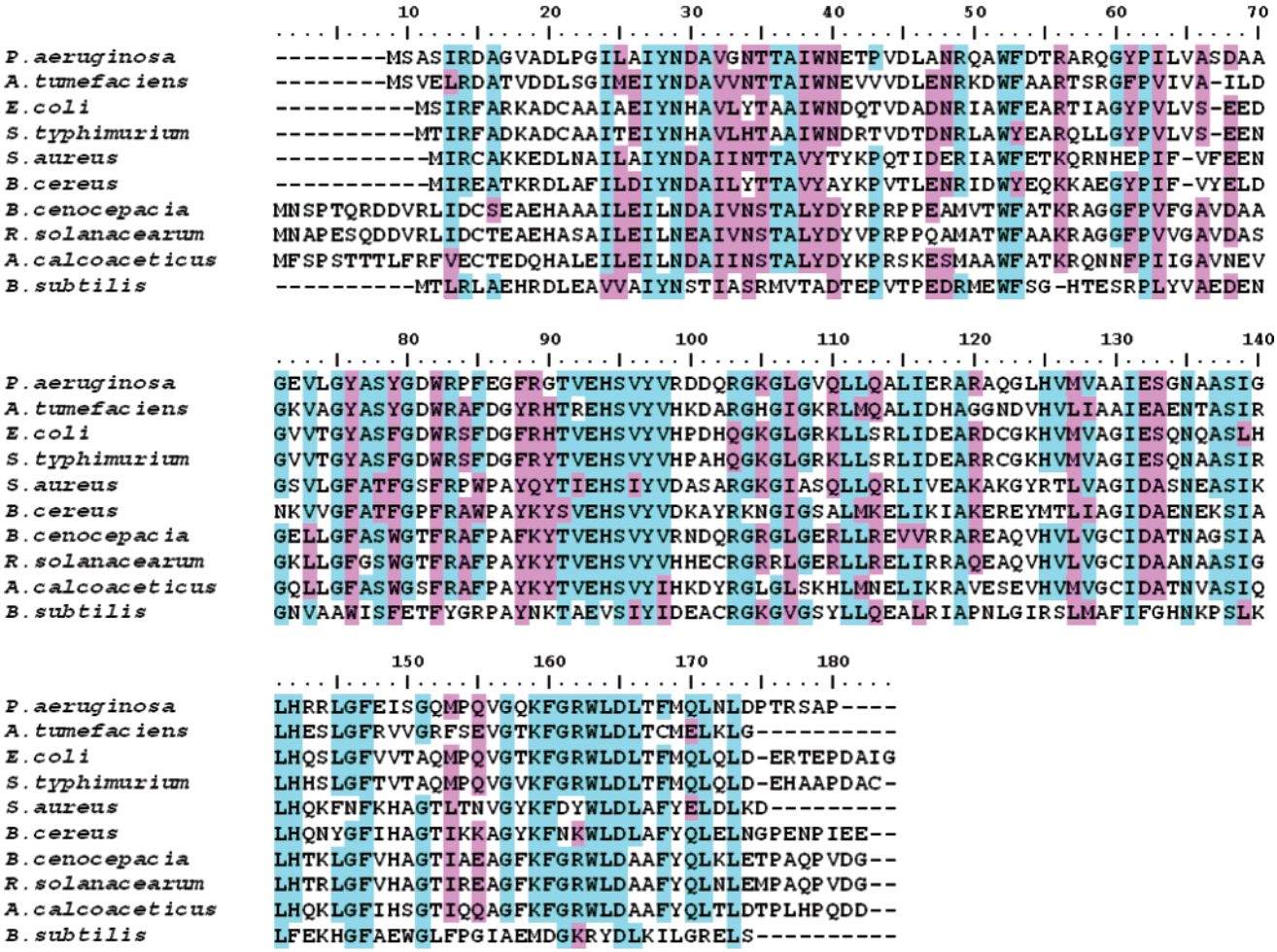

FIGURE 1: Multiple sequence alignment of a selection of proteins showing high sequence homology to pita: *P. aeruginosa*, *Pseudomonas aeruginosa* conserved hypothetical protein/pita (PA4866 gene); *A. tumefaciens*, *Agrobacterium tumefaciens* phosphinothricin acetyltransferase (AGR_C_1654 gene); *E. coli*, *Escherichia coli* hypothetical acetyltransferase (G6759/yncA gene); *S. typhimurium*, *Salmonella typhimurium* putative acyltransferase (SC1587/yncA gene); *S. aureus*, *Staphylococcus aureus* acetyltransferase (GNAT) family protein (SAS2415 gene); *B. cereus*, *Bacillus cereus* phosphinothricin *N*-acetyltransferase (NP_832560 gene); *B. cenocepacia*, *Burkholderia cenocepacia* undefined product (BCAL1022 gene); *R. solanacearum*, *Ralstonia solanacearum* antibiotic resistance (acetyltransferase) protein (RS00470 gene); *A. calcoaceticus*, *Acinetobacter caloaceticus* putative antibiotic resistance protein (Q6FBS8 gene); *B. subtilis*, *Bacillus subtilis* putative phosphinothricin *N*-acetyltransferase (B70064/YwnH gene). Residues colored in light blue are identical while those colored in light pink display 70% conservation. The multiple sequence alignment was performed using CLUSTAL W (*6*), and the figure was generated with BioEdit (*7*).

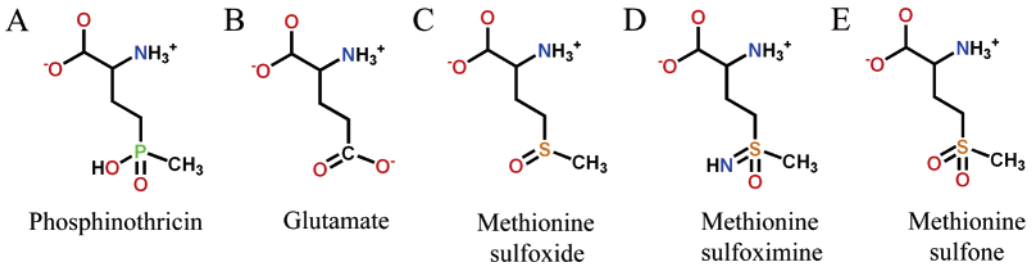

FIGURE 2: Chemical structures: (A) phosphinothricin; (B) glutamate; (C) methionine sulfoxide; (D) methionine sulfoximine; (E) methionine sulfone. The figure was drawn with ChemDraw Pro 8.0.

Å) crystal structure of pita in complex with one of its substrates, L-metsox, which revealed its mode of binding in the active site. We have also solved the structure of the apoenzyme (at room temperature), revealing that certain conformational changes occur in the active site upon substrate binding. As a result of examining the growth properties of a mutant strain, Depp4, that lacks pita activity, we propose a role for the enzyme in protecting *P. aeruginosa* against inactivation of its GS by L-metsox.

MATERIALS AND METHODS

Pita Purification. The pita gene (PA4866) was cloned into pET24a (*1*). *Escherichia coli* strain BL21(DE3) [pET24a (pita)] was grown overnight in 500 mL of LBkan medium with 1 mM IPTG at 37 °C. Cells were harvested by centrifugation, and pita was purified as described previously (*1*).

Sedimentation Equilibrium Studies. Sedimentation equilibrium experiments were carried out at 4 °C in a Beckman Optima XL-A analytical ultracentrifuge as described previously (*11*). Pita was dialyzed into PBS-azide (140 mM NaCl, 1.5 mM KH_2PO_4, 8.1 mM Na_2HPO_4, pH 7.4, plus 0.05% sodium azide) and loaded at concentrations corresponding to initial A_{280} values of 0.4−0.8. Data were collected at 11000, 13500, and 16000 rpm, as an average of 25 absorbance measurements at 280 nm, with a radial interval of 0.001 cm. The data at equilibrium were analyzed in terms of a single ideal solute to obtain the buoyant molecular mass $M(1-\bar{v}\rho)$ as previously described (*12*). The molecular mass was calculated using the previously determined solvent density (*12*) and a value of $\bar{v}$ of 0.7247 calculated from the amino acid composition using SEDNTERP (http://www.rasmb.bbri.org/).

Kinetic Studies. Assays for *N*-acetyltransferase activity were based on the method of D'Halluin et al. that follows at 412 nm the formation of the yellow 5-thio-2-nitrobenzoic acid produced by the reaction between 5,5′-dithiobis(2-nitrobenzoic acid) (DTNB) and the exposed −SH group of the reaction product, CoASH (*13*). Reactions were carried out at 37 °C in 50 mM Tris buffer, pH 7.2, and DTNB (4 mg/mL) in a volume of 0.9 mL. Absorbance changes were measured with a Pye Unicam SP8-400 spectrophotometer.

$K_{m(app)}$ determinations for L-metsox and L-metsone were made over the concentration ranges 28−0.08 mM (20−0.08K_m) and 7−0.15 mM (7−0.15K_m), respectively, at near-saturating acetyl-CoA (0.5 mM). $K_{m(app)}$ values for acetyl-CoA were measured over a concentration range (0.5−0.006 mM) (12−0.07K_m) at near-saturating concentrations of L-metsox (20 mM). Measurements were made in duplicate, and data were fitted to the equation $v = V_mS/(K_m + S)$ using the Leonora program (*14*). Molar extinction coefficients for 5′-thio-2-dinitrobenzene and pita (monomer) were 13600 at 412 nm and 29160 at 280 nm (*15*), respectively.

Bacterial Strains, Plasmids, and Media. P. aeruginosa strain PAC1 (8602) (*16*) is the parent of strain Three, a urease-minus mutant harboring a mutation, A166V, in the *ureC* gene (PA4868) product (*17*) that inactivates urease and prevents utilization of urea as a nitrogen source. Strain Depp4 is derived from strain Three and contains an in-frame deletion in the pita gene engineered as described in this paper.

Minimal media were prepared from minimal salt media (*18*). Sodium succinate (S) [0.5% (w/v)] provided the carbon source, and the nitrogen sources urea (U), ammonium chloride (N), proline (Pro), glutamate (Glu), and glutamine (Gln) were at 0.1% (w/v). Antibiotic concentrations were as follows: carbenicillin, 400 μg/mL; kanamycin sulfate, 50 μg/mL. *Pseudomonas* isolation agar was from Difco. pET24a was from Novagen. Plasmids pSWkan and pSW(SceI) (*19*) were a gift from Dr. Sandy Wong.

Construction of Pita Deletion Strain Depp4. The region of the pita gene targeted for deletion was between bases G316−C351 corresponding to amino acid residues A106−H117. The 36 bp deletion was created adjacent and 3′ to an existing *Pst*I site, and the method used, a modification of one described by Wong and Mekalanos (*19*), is shown in Figure 3. PCR primers (Table 1) were designed to amplify DNA regions on either side of the intended deletion. The upstream region (amplified by primers EF and Inner) extended from the middle of the *ure*D gene (complementary to primer EF) to the region 5′ to the *pita* deletion. The downstream region extended from the middle of the *ure*C gene, corresponding to primer Rex, to the region immediately 3′ to the deletion, corresponding to primer IF. Primers Inner and IF each incorporated a *Pst*I site at their 5′ ends. After PCR amplifications with primer pairs EF/Inner and IF/Rex using *P. aeruginosa* PAC1 chromosome as template, the products were cut with *Pst*I and gel purified. The two PCR fragments were ligated, and an aliquot of the ligated product was amplified using the primers EF and Rex. After gel cleaning and end-filling, the product was cloned into the

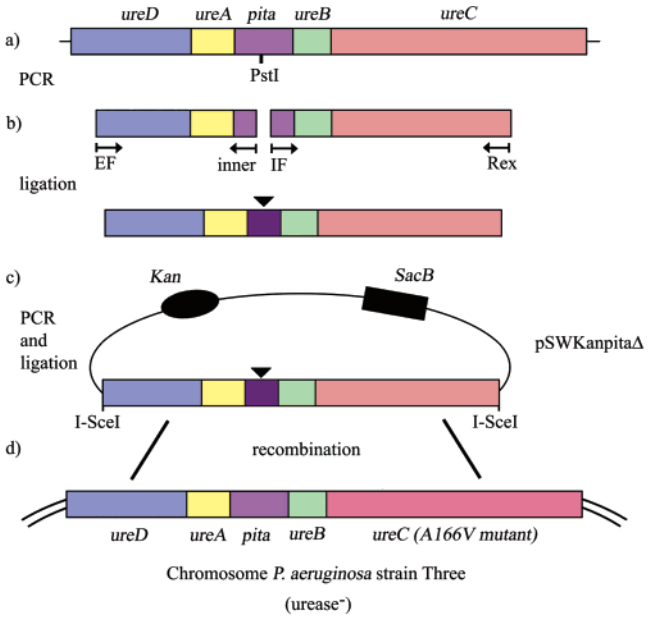

FIGURE 3: Construction of strain Depp4 with a chromosomal deletion in pita [adapted from Wong and Mekalanos (*19*)]. The deleted DNA region corresponding to A106−H117 in pita lies immediately downstream of a *Pst*I site. Primers IF and Inner each incorporated a *Pst*I site within their 5′ ends, IF primed at the original *Pst*I site, Inner primed from 36 bases upstream of the original site. The PCR products from EF/Inner and IF/Rex were cut with *Pst*I and ligated to create the deletion and recreate a *Pst*I site. The ligated product was amplified by PCR using EF/Rex primers and cloned into the *Sma*I site of pSWkan where it was flanked by 18 bp recognition sequences for I-SceI. This plasmid pSWkan(pitaΔ) was introduced into strain Three that carries a urease-negative mutation A116V in the *ureC* gene product. Strain Three also harbored the carbenicillin resistance encoding plasmid pSW (I-SceI) that expresses I-SceI to allow the insert to be released from pSWkan-(pitaΔ), increasing the frequency of its recombination with the homologous region of the chromosome. Selection was finally made for colonies able to grow S/U medium in the presence of 5% sucrose. This selects for urease-positive recombinants that have lost the pSWkanpitaΔ plasmid because SacB expression prevents growth in the presence of sucrose (*20*). These were then screened by PCR for the presence of the deletion.

Table 1: PCR Primers

primer	sequence
EF	5′-ACCGCTGCGAGCTCAGAAGCACCTCTACGCCGA-3′
Inner	5′-AAAACTGCAGCAGTTGCACGCCGA-3′
AF	5′-GAGTACCTGAGATGGACTTGT-3′
Rex	5′-GTCGGTCTAGATCGCCACCTGGATGTCGTGGCGCT-3′
IF	5′-AAAACTGCAGGTCATGGTGGCCGCCATCGA-3′
PAGSF	5′-GGAGGACCATATGTCGTACAAGTCGCACCA-3′
PAGSR	5′-GGAAAGGGATCCTCAGACGCTGTAGTACAGGT-3′
PitapetF	5′-TGAGGCCGCATATGAGCGCTTCGATCCGCGACG-3′
PitapetR	5′-TTCACCGGGATCCATGGGGGCTCCTTGGGCTCA-3′
Brev	5′-GACCTCTAGAGTTGGGAACGGGCCCTAGAGGT-3′

*Sma*I site of pSWkan to give pSWkan(pitaΔ). The recombinant plasmid was introduced into *E. coli* S17.1 by electroporation. *E. coli* S17.1 (pSWSce1) was used to introduce pSWSce1 into *P. aeruginosa* PAC1 urease-negative mutant, strain Three, by plate mating overnight at 37 °C on LB medium. Transformants were selected by subsequent patching onto *Pseudomonas* isolation agar containing carbenicillin. *P. aeruginosa* strain Three (pSWSceI) grown overnight in LB carbenicillin medium and S17.1 (pSWpitaΔ)) grown overnight in LBkan medium were each resuspended in LB medium, mixed, and grown together on LB solid medium at 37 °C overnight. The cells were washed in 50 mM phosphate buffer, pH 7.2, and plated on S/U medium containing 5% (w/v) sucrose. Colonies appearing after a few days of growth at 37 °C were streaked on the selection medium. To check that the deleted pita gene was present in the *Pseudomonas* chromosome, the selected colonies were analyzed by PCR using a forward primer (AF) designed to correspond to a sequence within the open reading frame upstream of the *ure*A gene and Brev, that primes within the *ure*B gene as reverse primer. Two out of 6 colonies gave a smaller PCR product than the one obtained using the wild-type chromosome as template. The PCR product from one of the strains, Depp4, was sequenced to confirm the deletion. Repeated subculturing of Depp4 on LB medium was used to lose pSWSceI. To clone the *pita*Δ gene, chromosomal DNA from strain Depp4 was used as a PCR template with pita gene primers pitapetF and pitapetR. After cutting the PCR product and vector with *Nde*I and *Bam*HI, *pita*Δ was subcloned into pET24a.

Growth Inhibition Studies. Bacteria were grown overnight in 5 mL of LB at 37 °C, washed with 50 mM phosphate buffer, pH 7.2, and then resuspended in 5 mL buffer, and 0.1 mL was used to inoculate 50 mL of the appropriate medium in 250 mL flasks. Cultures were grown in a rotary shaking incubator at 200 rpm, 37 °C. L-Metsox was added when cultures had entered log phase, and growth was monitored by measuring the optical density of samples at A_{600nm}.

Selection of L*-Metsox-Resistant Mutants of Strain Depp4.* Strain Depp4 was grown in 5 mL of LBkan medium and washed, and 0.1 mL was plated on S/U solid medium containing 5 mM L-metsox. Colonies were picked off after 48 h incubation at 37 °C and then purified by restreaking on the isolation medium. Four mutant strains, XN1−4, were retained for further study.

PCR Amplifications. PCR amplifications were routinely carried out using 50 μL of Red Taq Readimix (Sigma) containing *P. aeruginosa* chromosomal DNA as template and primer concentrations of 0.2 μM; 0.5 μL of *Pfu*I (Promega) was included in the mixture. The program was 30 s at 94 °C followed by 30 cycles of 30 s at 94 °C, 30 s at 58 °C, and 1 min at 72 °C. Conditions for PCR amplification of the *gln*A genes (PA5119) of strains XN1 and XN4 were the same but using primers PAGSF/PAGSR and an extension time of 1 min 30 s.

To create the pita gene deletion, PCR reaction mixtures contained EF/Inner and IF/Rex primer pairs, respectively, in addition to Polymix (Bioline Ltd.), 50% (v/v), and 1 μL of *Pfu*I/100 μL. The amplification program was as above but with the extension time increased to 2 min 5 s. After digestion with *Pst*I and gel cleaning, 100 ng of PCR products in equimolar amounts was ligated with 1 μL of T4DNA ligase in 10 μL. For production of the PCR product from the ligated PCR fragments using EF/REX primers, the PCR mix contained 50% Polymix and 0.5 μL of long enzyme (Bioline)/100 μL mixture with 1 μL of the ligation mixture as template. The extension time was 1 min 20 s.

Table 2: Data Processing Statistics

dataset	HR	RT	METSOX
space group	$P2_12_12_1$	$P2_12_12_1$	$P2_12_12_1$
unit cell dimensions			
a (Å)	47.749	47.967	47.637
b (Å)	56.868	57.522	57.197
c (Å)	124.470	126.736	125.179
resolution limit (Å)	1.44	2.35	1.55
no. of unique reflections	58095	14726	49827
outer shell (Å)	1.48−1.44	2.41−2.35	1.59−1.55
completeness (%), overall (outer shell)	93.8 (93.8)	97.2 (97.2)	98.9 (90.7)
multiplicity, overall (outer shell)	2.8 (2.7)	4.5 (4.4)	6.7 (4.9)
I/σ, overall (outer shell)	11.6 (3.5)	15.7 (5.8)	16.0 (3.1)
R_{merge} (%), overall (outer shell)	4.4 (34.2)	10.5 (26.6)	11.6 (38.8)

Crystallization. Pita crystals were grown using the hanging drop vapor diffusion method. The reservoir solution contained 500 μL of 100 mM sodium cacodylate at pH 6.5 or 100 mM Tris-HCl at pH 7.5, 18−22% (w/v) PEG 10000, and 0.1% (w/v) NaN_3. The drops contained 1.5 μL of protein solution at a concentration of 10 mg/mL, to which an equal volume of reservoir was added. The drops were kept at a temperature of 291 K (±0.5 K). Crystals appeared after 1 day and grew to 1.5 mm in length, although the best quality crystals (i.e., those diffracting to high resolution) had typical dimensions of 100 μm × 100 μm × 500 μm.

For the high-resolution native structure (HR), the crystal was flash cooled in liquid nitrogen using reservoir solution containing 22% (v/v) glycerol. For the room temperature native structure (RT), the crystal was mounted in a quartz capillary. For the L-metsox complex structure (METSOX), the crystal was soaked in a solution containing reservoir solution, 22% (v/v) glycerol, and 50 mM L-metsox for 1 min before flash cooling in liquid nitrogen.

Data Collection and Processing. Data for the HR structure were collected at Stn14.2, Synchrotron Radiation Source (SRS), Daresbury, U.K. (λ = 0.98 Å, d = 100 mm, temperature = 100 K). Data for the RT structure were collected in-house [(λ = 1.54 Å, d = 190 mm, temperature = 293K) (Elliott Bros Ltd. GX18 rotating anode generator operating at 45 kV/45 mA, Rigaku MSC R-AXIS4^{++} detector, Osmic mirrors)]. Data for the METSOX structure were collected at Stn10.1, SRS (*21*) (λ = 0.98 Å, d = 155 mm, temperature = 100 K). The data were processed with DENZO (*22*) (RT and HR datasets) and MOSFLM (*23*) (METSOX dataset) and the CCP4 suite of programs (*24*). Data processing statistics are summarized in Table 2.

Structure Determination. All structures were solved by molecular replacement using MOLREP from the CCP4 suite of programs (*24*, *25*). The HR structure was solved using protein atoms from 2BL1 (*1*) as a starting model. The RT and METSOX structures were solved using the refined HR structure as a starting model.

Model Building and Refinement. Refinement was performed using CNS (*26*). Cycles of refinement were alternated

Table 3: Refinement Statistics

dataset	HR	RT	METSOX
resolution range (Å)	56.79−1.44	63.25−2.35	47.62−1.55
no. of reflections	58095	14726	49827
no. of protein atoms (per asymmetric unit)	2713	2609	2713
no. of water molecules (per asymmetric unit)	565	180	626
average *B* factor (Å^2)			
for protein atoms	14.10	27.62	13.02
for water molecules	26.53	38.98	30.51
for L-metsox			21.82 (mol A) 18.77 (mol B)
R_{cryst} (%) (all reflections)	19.94	18.88	18.00
R_{free} (%) (5% of reflections)	20.82	22.42	21.30
σ_A coordinate error (Å)	0.18	0.27	0.15
rmsd, bond lengths (Å)	0.007	0.007	0.011
rmsd, bond angles (deg)	1.36	1.40	1.36

with rounds of manual model building with QUANTA (*27*) using σ_A-weighted $2|F_o| - |F_c|$ and $|F_o| - |F_c|$ electron density maps. Noncovalently bound species (water and glycerol molecules, azide ions, and L-metsox) were incorporated into the structures after protein atoms had been modeled. An L-metsox molecule [2-amino-4-(*S*-methylsulfonimidosyl)butanoic acid] (for the METSOX structure) was built in QUANTA (*27*) using coordinates for phosphinothricin (*28*) as a template. Bond angles and lengths were adjusted to agree with values observed in the methionine sulfoximine crystal structure (*29*). CNS topology and parameter files for L-metsox were generated using the PRODRG server (*30*). Other ligand topology and parameter files used for refinement were obtained from the HIC-Up database (*31*). Five percent of the reflections were used to calculate the R_{free} value throughout the refinement process, with the exception of two final rounds of refinement where all reflections were used. The two NCS-related molecules of the asymmetric unit (termed A and B) were refined independently. The final models were analyzed using PROCHECK (*32*), SFCHECK (*33*), CNS (*26*), and Coot (*34*). Secondary structures were assigned using the DSSP server (*35*), and structural superpositions were performed using the DALI Lite server (*36*). Refinement and final model statistics are summarized in Table 3. Atomic coordinates and structure factors have been deposited in the Protein Data Bank (*37*) with the following codes: HR, 2J8M; RT, 2J8N; METSOX, 2J8R.

RESULTS

Sedimentation Equilibrium Studies. The sedimentation equilibrium data can be modeled to single ideal species, with the residuals of the fit randomly distributed around zero (Figure 4). The average buoyant molecular mass [$M(1 - \bar{v}\rho)$] for the various speeds and concentrations was 10536 ± 354. Using an experimentally determined solvent density (*12*) and a partial specific volume estimated from the sequence, the molecular mass obtained is 39011 ± 1311. The molecular mass calculated from the sequence is 18713 for a monomer and 37426 for a dimer, so it is clear that pita dimerizes in solution.

Properties of Purified Pita. No acetyltransferase activity was detected for pita using DL-phosphinothricin as substrate

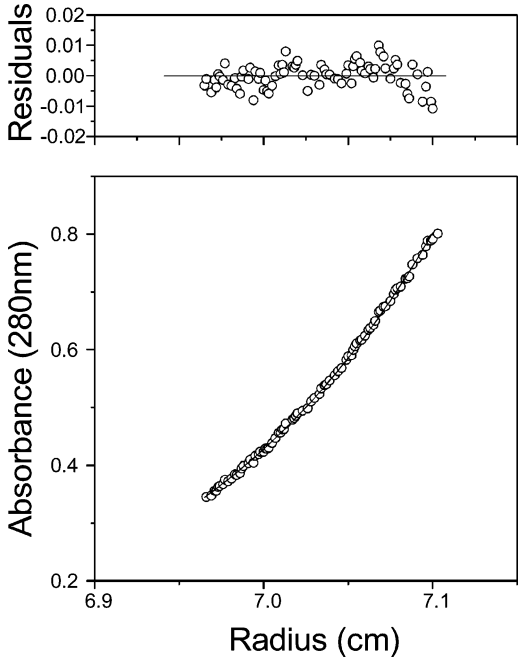

FIGURE 4: Pita is dimeric in solution. Sedimentation equilibrium data for pita shown as a distribution of A_{280} at equilibrium. A representative data set is shown at 13500 rpm. The results are analyzed for the best single-component $M(1 - \bar{v}\rho)$ fit, shown as a line through the experimental points, with the residuals shown above. The value of $M(1 - \bar{v}\rho)$ of 10536 ± 354, and therefore molecular mass of 39011 ± 1311, indicates that the protein is a dimer under the experimental conditions.

Table 4: Kinetic Parameters for *P. aeruginosa* Pita

substrate	$K_{m(app)}$ (mM)	$k_{cat(app)}$[a] (s^{-1})
L-methionine sulfoximine	1.3 ± 0.21[b]	505 ± 43[b]
L-methionine sulfone	1.3 ± 0.13[b]	610 ± 23[b]
acetyl-CoA	0.03 ± 0.0008[b]	

[a] $k_{cat(app)}$ values are based on one active site per pita monomer. [b] Result is the mean ± SEM.

with up to 1 mg of purified enzyme in the 0.9 mL standard assay mixture. Other glutamate analogues, L-metsone and L-metsox, were substrates, and determination of kinetic parameters showed that both compounds had similar $K_{m(app)}$ and $k_{cat(app)}$ values (Table 4). DL-Methionine sulfoxide, L-methionine, and L-glutamate were not substrates. No inhibition of pita activity was observed with 20 mM phosphinothricin in the enzyme assay mixture with a range of concentrations of L-metsox from 0.17 to 3.8 mM.

Properties of the Depp4 Pita Deletion Strain. To investigate the function of pita, a mutant strain, Depp4, with a 36 bp in-frame deletion in the *pita* gene, was made. DNA sequencing confirmed the deletion and showed that the mutation (responsible for A166V) in the *ure*C gene in the parental strain, Three, had been converted back to wild type. To check that the deletion had knocked out pita activity, the *pita*Δ gene from Depp4 was cloned into pET24a, and the recombinant plasmid was used to transform *E. coli* strain BL21(DE3). Extracts of a transformant after growth on LBkan with IPTG had no detectable pita activity, neither was there a protein detectable by SDS−PAGE corresponding to the expected size of pita. We concluded that the deletion had eliminated activity and resulted in degradation of the protein. Depp4 grew in S/U and S/N media with the same

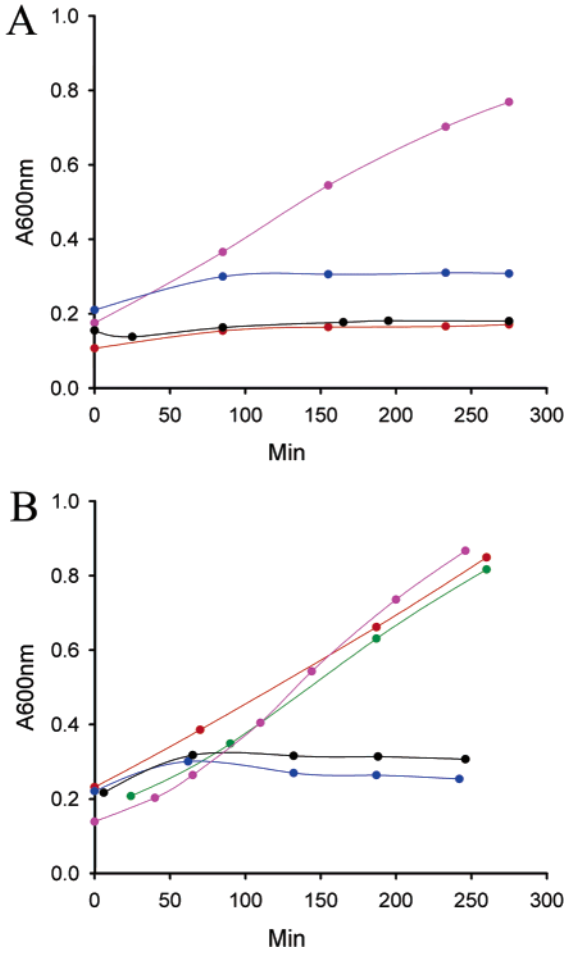

FIGURE 5: Growth inhibition of strain Depp4 by L-metsox. (A) Effect of the nitrogen source on growth inhibition of strain Depp4 by L-metsox: S/Gln + 0.2 mM L-metsox (pink), S/Glu + 0.2 mM L-metsox (blue), S/Pro + 0.2 mM L-metsox (red), and S/U + 0.1 mM L-metsox (black). L-Metsox was added to growing cultures at 0 min. (B) Comparison of the effects of L-metsox on the growth of *P. aeruginosa* strains 8602, Three, and Depp4 on S/N medium: 8602 + 0.5 mM L-metsox (red), Three + 0.5 mM L-metsox (green), Depp4 + 0.5 mM L-metsox (blue), Depp4 + 0.005 mM L-metsox (black), and 8602 without L-metsox (pink). L-Metsox was added to the growing cultures at 0 min for strains 8602 and Depp4 and at 24 min for strain Three.

doubling times, 129 and 55 min, respectively, as the wild-type strain, PAC1.

Role of Pita. The growth of Depp4, its parent strain Three, and the wild-type organism, PAC1, was compared to see if inactivation of pita affected the ability of Depp4 to utilize different nitrogen sources in the presence of L-metsox. Growth of Depp4 in succinate medium with glutamate, ammonium, urea, and proline as nitrogen sources was stopped by the addition of 200 μM L-metsox at the beginning of the log phase (Figure 5A), and no further growth was observed for the next 12 h. Growth with glutamine as a nitrogen source was unaffected (Figure 5A). L-Metsox at 0.5 μM stopped the growth of Depp4 on S/U and S/N media (Tata and Brown, unpublished results). In contrast, 0.5 mM L-metsox had no effect on the growth of the wild-type strain PAC1 or strain Three on any of the nitrogen sources (data shown for S/N in Figure 5B). L-Metsox-inhibited cultures of strain Depp4 were analyzed for viability by serial dilution and colony counting on nutrient agar. The results showed that cells were viable, indicating that L-metsox was acting as a bacteriostatic agent. Phosphinothricin, applied as crystals to strains PAC1 and Depp4 growing as lawns on solid minimal media, had no discernible inhibitory effect on growth.

L-Metsox- Resistant Strains Obtained from Depp4. Mutant strains were obtained from strain Depp4 that grew on S/N solid medium containing 5 mM L-metsox. Four colonies, mutant strains XN1−XN4, were purified and their properties investigated. All grew on S/N and glutamine solid media, but XN1 and XN4 were unable to grow on S/U medium. Sequencing of the PCR-amplified *glnA* genes encoding glutamine synthetase (GS) from these two strains showed that both harbored single base changes, T641A (XN1) and G640A (XN4), translating as mutations V214E and V214M, respectively, in GS.

Overall Fold. The overall folds of the structures described in this paper are essentially identical to that previously described for pita (ref *1* and Figure 6A), which was found to be similar to that of the YwnH protein from *B. subtilis* (*2*) (PDB code 1VHS; 29% sequence identity; rmsd 1.7 Å, Cα atoms). Recently, structures have also been solved for pita from *P. aeruginosa* strain PAO1 (PDB code 1YVO; 98% sequence identity; rmsd 0.4 Å, Cα atoms) and the AGR_C_1654 protein from *A. tumefaciens* (PDB code 1YR0; 59% sequence identity; rmsd 0.7 Å, Cα atoms). The folds of these proteins are all remarkably similar, and there is a high degree of residue conservation in the active sites of pita and AGR_C_1654 in particular. While sharing a similar fold to pita and AGR_C_1654, there is a lower degree of residue conservation in the active site of YwnH from *B. subtilis*.

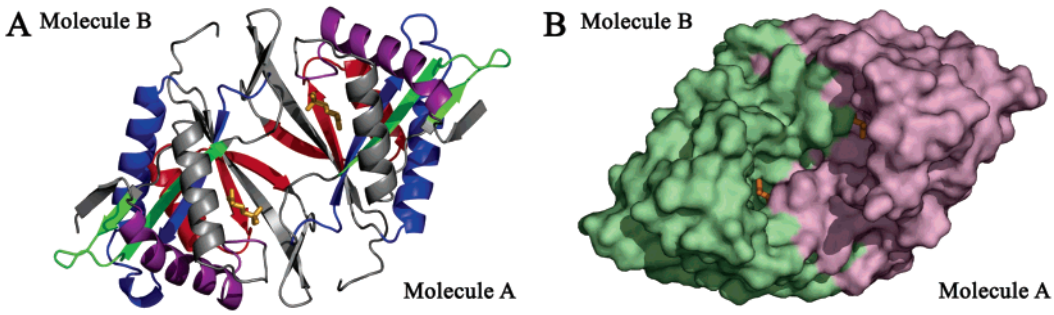

FIGURE 6: (A) The pita dimer. Molecules A and B of the asymmetric unit are shown. The GNAT motifs defined by Neuwald and Landsman (*38*) are colored, from N to C terminus, as follows: purple (motif C), green (motif D), blue (motif A), and red (motif B). L-Methionine sulfoximine is colored in orange. All other atoms are colored in gray. (B) Surface representation of the pita dimer. Protein atoms of molecules A (purple) and B (green) of the METSOX structure are shown, and their orientation is the same as that in Figure 6. L-Methionine sulfoximine (orange) binds at one end of a channel running through the center of the protein. The figure was generated with PyMOL (*39*).

Dimerization. The sedimentation equilibrium data presented above clearly show that pita exists as a dimer in solution. In the orthorhombic crystal form of pita discussed here there are two molecules in the crystallographic asymmetric unit (Figure 6), arranged in a remarkably similar manner to other dimeric GNAT superfamily members such as the *Saccharomyces cerevisiae* glucosamine-6-phosphate *N*-acetyltransferase GNA1 (*40*), *Enterococcus faecium* aminoglycoside acetyltransferase AAC(6′)Ii (*41*), and *Salmonella typhimurium* RimL N^{α}-acetyltransferase (*42*).

The two pita subunits are related to one another by a 2-fold rotation axis, burying an area of approximately 3100 Å^2 at an interface which is almost entirely devoid of water molecules. One interesting interaction between the two molecules involves ring stacking between His117 of molecule A, Trp155 of molecule B, and the C-terminal proline residue (Pro172) of molecule A (and vice versa in the other molecule). Importantly, the two molecules also interact with one another in their active sites. This interaction is also present in the tetragonal crystal form of pita [PDB code 2BL1 (*1*)] where the single molecule of the asymmetric unit forms a dimer with another, symmetry-related molecule.

Due to the extensive interaction between the two molecules of the asymmetric unit (including residues located in the active site) and the similarity of this arrangement compared with other dimeric acetyltransferases, we believe the pita dimer presented here to be the enzyme's physiological state.

Binding of L*-Metsox in the Active Site (METSOX Structure).* L-Metsox was found to bind in the active site of both molecules in the asymmetric unit, with the binding sites separated by a distance of approximately 20 Å. The location of the binding sites in the pita dimer is shown in Figure 6. L-Metsox was bound in an essentially identical manner in both molecules, and discussion of its mode of interaction with the enzyme will therefore be limited to molecule B. Electron density for L-metsox in the pita active site is shown in Figure 7A.

Part of the tetrahedrally shaped methylsulfonimidosyl group of the substrate is positioned above the indole group of Trp31 (from molecule B), inclined at an angle of ~25° relative to the indole group plane. The protonated nitrogen atom and oxygen atom of the methylsulfonimidosyl group lie closest to the pyrrole ring of the indole group at distances of 3.4 Å (N−Nϵ2) and 4.8 Å (O−Cδ2), respectively. The oxygen atom also lies 2.9 Å away from the guanidinium group of Arg75 (from molecule A) and is in a favorable position to form a hydrogen bond with this residue. On the other hand, the methyl portion of the methylsulfonimidosyl group does not lie above the pyrrole ring and instead lies ~3.7 Å away from Ile30 (molecule B) and Phe77 (molecule A), which together form a hydrophobic surface interacting with this portion of the substrate (Figure 7A,B). Both molecules of the pita dimer clearly play a role in interacting with the methylsulfonimidosyl group of the substrate and in shaping part of the substrate binding site. It is also clear that active site residues are important for formation of the dimer as Arg75 from molecule A is able to form a salt bridge with Glu85 from molecule B.

Only residues from molecule B lie close to the substrate's carboxyl and amino groups. It was somewhat surprising that these two functional groups did not form any specific interaction with residues in the active site. However, the active site is exposed to solvent, and these groups are able instead to form hydrogen bonds with nearby water molecules, with an average hydrogen bond length of 2.7 Å. In particular, the carboxyl group forms a hydrogen bond with a water molecule, which is in turn hydrogen bonded to Tyr89 from molecule B (Figure 7A).

Substrate Binding Causes a Conformational Change. In the HR structure, it was found that a glycerol molecule (resulting from the use of glycerol as a cryoprotectant) had bound in the active site of both molecules of the asymmetric unit, in an equivalent position to that of the methylsulfonimidosyl portion of L-metsox in the METSOX structure. Superposition of the Cα atoms of these structures revealed that the conformations adopted by Ile30 and Tyr89 in the HR structure were different from those in the METSOX structure. However, to study the active site and investigate its flexibility in the complete absence of a small molecule, a dataset was collected at room temperature (RT structure).

Comparison of the METSOX, HR, and RT structures revealed that Ile30 and Tyr89 adopted essentially identical conformations in the HR and RT structures (which were different from those in the METSOX structure). The RT structure also revealed that Trp31 undergoes a considerable conformational change when substrate is bound in the active site, a change that was not observed in the HR structure in which the glycerol molecule had bound in an equivalent position to the methylsulfonimidosyl portion of L-metsox.

The conformational changes associated with substrate binding (shown in Figure 7C) will be discussed with reference to the RT and METSOX structures. In the METSOX structure, Ile30 was found to undergo a 110° clockwise rotation about its C−Cα−Cβ−Cγ1 (χ_1) torsion angle, followed by a 110° rotation about its Cα−Cβ−Cγ1−Cδ1 (χ_2) torsion angle, helping to create a hydrophobic surface for the methylsulfonimidosyl portion of the substrate. Tyr89 moves away from the active site, allowing a water molecule to bind and form a hydrogen bond mediated bridge between the hydroxyl of Tyr89 and the carboxylate group of the substrate (Figure 7A). In the RT structure, the Oγ atom of Ser87 (a highly conserved residue among the pita-like enzymes; residue numbered 95 in Figure 1) points away from the active site. However, in the HR and METSOX structures, Ser87 adopts two conformations (Figure 7). If adoption of these two alternative conformations were indicative of disorder in the active site, then Ser87 might also have been expected to behave similarly in the RT structure. The adoption of a single conformation by Ser87 in the RT structure suggests that the presence of a second conformer may be correlated with a small molecule binding in the active site. However, the role of Ser87 is not yet clear as this residue was not found to form any specific interactions with the substrate.

The most pronounced difference between the active sites of the RT and METSOX structures is the conformation adopted by Trp31 (Figure 7C). In order to accommodate the substrate in the active site, Trp31 undergoes a rotation about its Cα−Cβ−Cγ−Cδ1 (χ_2) torsion angle, such that the plane of the indole group rotates by ~60° anticlockwise.

DISCUSSION

To summarize the structural data presented here, we have solved the structure of pita with a dimer in the asymmetric

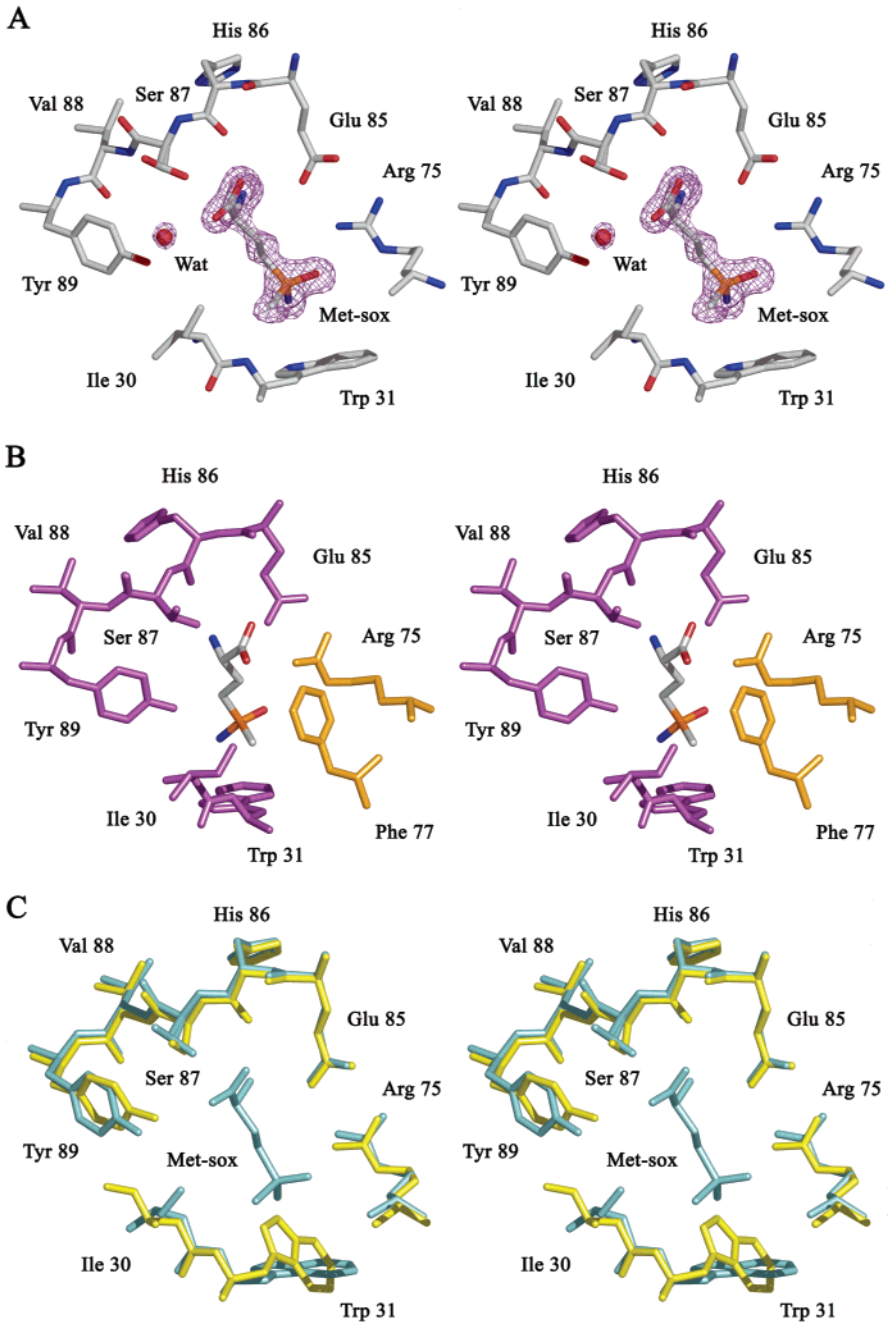

FIGURE 7: (A) Electron density for L-methionine sulfoximine. A stereoview of the active site from molecule B of the METSOX structure is shown. Density is shown using a σ_A-weighted $2F_o - F_c$ electron density map and is contoured at 1.0σ. (B) Substrate binding involves both molecules of the dimer. The orientation is the same as that in panel A after rotation about a vertical axis in the plane of the paper. Arg75 and Phe77 from molecule A (orange) protrude into the active site of molecule B (residues colored in purple) and form a hydrophobic interaction with the methylsulfonimidosyl portion of the substrate. Arg75 forms a hydrogen bond to the substrate and also to Glu85 from molecule B. Ser87 adopts an alternative conformation, with the alternative conformer oriented toward the substrate. (C) Substrate binding causes a conformational change. A stereoview of molecule B of the RT (yellow) and METSOX (light blue) structures is shown. Upon substrate binding, Ile30 and Trp31 undergo a conformational change involving rotation about their side chain torsion angles. Tyr89 moves away from the active site, and Ser87 adopts an alternative conformation. The figure was generated with PyMOL (*39*).

unit (in agreement with analytical ultracentrifugation studies), in both the native form and in complex with a substrate. We have demonstrated that a conformational change occurs upon substrate binding and how residues from both molecules of the dimer contribute in forming the active site.

Substrate Specificity. L-Metsox and L-metsone are substrates for pita whereas phosphinothricin, L-methionine sulfoxide, and L-glutamate are not. The METSOX structure revealed the mode of interaction between pita and L-metsox, showing how the tetrahedrally shaped methylsulfonimidosyl portion of the substrate formed interactions with certain active site residues. Presumably, L-metsone, with its tetrahedrally shaped methylsulfonyl group, would bind in a similar manner to L-metsox. While L-methionine sulfoxide and L-glutamate share some similarities in the functional groups in the region corresponding to the methylsulfonimidosyl groups of L-metsox (Figure 2), these groups would possess distorted tetrahedral and trigonal geometry, respectively, and may therefore be unable to interact with the enzyme in a favorable manner.

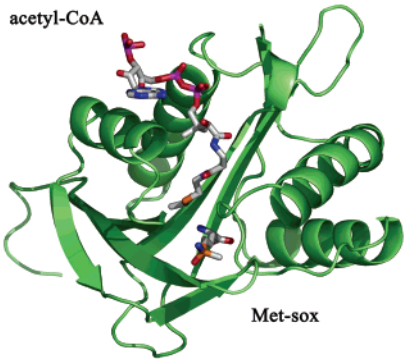

FIGURE 8: Predicted acetyl-CoA binding site. The predicted binding site of acetyl-CoA is shown after superposition of molecule B of the METSOX structure onto that of the tabtoxin resistance protein [PDB code 1GHE (*43*)]. Molecule B of the METSOX structure is colored green, and the position of L-metsox is shown. For clarity, protein atoms from 1GHE are not shown. The figure was generated with PyMOL (*39*).

It is more intriguing to consider why pita is unable to utilize phosphinothricin as a substrate, given its structural and, to a certain extent, chemical similarity to L-metsox, reflected in the ability of both to act as GS inhibitors (*28*). The only chemical differences between these compounds are that the sulfur atom and protonated nitrogen of the methylsulfonimidosyl portion of L-metsox are replaced in phosphinothricin by a phosphorus atom and hydroxl group, respectively. The mode of L-metsox binding in the pita active site does not provide any immediate clues as to why phosphinothricin is not a substrate, and this aspect of pita's substrate specificity requires further investigation. However, comparison of pita's sequence with that of the *Streptomyces* phosphinothricin acetyltransferase revealed that there are differences in certain residues responsible for substrate binding, which may affect specificity. Residues which shape one part of the substrate binding site in pita (Arg75, Glu85, His86, Ser87, Val88, and Tyr89) are conserved in the *Streptomyces* enzyme (Lys, Glu, Ser, Thr, Val, and Tyr, respectively). Trp31 in pita is also conservatively substituted, replaced by Phe. However, Ile30, which forms a hydrophobic interaction with the methyl group of L-metsox, is replaced by Asn in the *Streptomyces* enzyme. While phosphinothricin also contains a methyl group, it is possible that this particular residue difference is able to affect the mode of substrate binding in the active site, in addition to substrate specificity.

Attempts were made to cocrystallize pita in the presence of phosphinothricin, as well as soaking phosphinothricin into pita crystals to determine whether it could bind in pita's active site, but neither method was successful. This apparent lack of binding of phosphinothricin was consistent with the observation that it is neither a substrate nor an inhibitor of pita.

Binding of Acetyl-CoA. Attempts were made to soak acetyl-CoA into existing pita crystals and to cocrystallize pita in the presence of acetyl-CoA in order to study the nature of its binding to the enzyme. Unfortunately, neither of these approaches was successful as crystals soaked in acetyl-CoA were found to crumble within 1 min, and screening for cocrystallization conditions did not yield any positive hits.

In order to gain insight as to how acetyl-CoA might bind to pita, the METSOX structure was superposed onto that of the tabtoxin resistance protein in complex with acetyl-CoA (PDB code 1GHE; 24% sequence identity; rmsd 2.0 Å, Cα atoms) (*43*). Despite low sequence similarity, the overall fold of the tabtoxin resistance protein was remarkably similar to that of pita. Pita has a channel running through its center, and L-metsox binds at one end of this channel (Figure 6). Comparison with 1GHE revealed that acetyl-CoA might bind at the other end of the central channel in pita. The shape of the channel is such that acetyl-CoA could adopt a similar conformation to that in 1GHE by bending at the pantetheine and pyrophosphate groups (*43*), placing its acetyl group approximately 3 Å from the amino group of L-metsox and therefore in a suitable position for N-acetylation of the substrate (Figure 8).

Comparison with 1GHE also provided insight as to why pita crystals soaked in acetyl-CoA crumbled, as the predicted location of the acetyl-CoA adenylyl group would disrupt contacts between protein molecules in the crystal.

A New Family of Enzymes? Structures have been solved for pita-like enzymes from *P. aeruginosa* strain PAC1 (ref *1* and this paper), *P. aeruginosa* strain PAO1 (PDB code 1YVO), *A. tumefaciens* (PDB code 1YR0), and *B. subtilis* (PDB code 1VHS), revealing a similar fold. There is a high degree of similarity between pita and its homologue from *A. tumefaciens*. Important active site residues such as Ile30, Trp31, Arg75, Phe77, Glu85, Ser87, and Tyr89 are all conserved, and their arrangements in the active site are similar. It is therefore likely that these two enzymes will share similar substrate profiles and belong to the same family.

On the other hand, the pita-like enzyme from *B. subtilis* displays a lower degree of sequence similarity to pita, and although some active site residues (Glu85, Ser87, and Tyr89) are conserved, others (Ile30, Trp31, Arg75, and Phe77), which are important for substrate interaction, are not. In addition, Trp31 is replaced by a Phe residue from a different part of the protein chain (residue 132 in Figure 1). Given these differences in the active site, it is likely that, despite sharing a similar fold, the pita-like enzyme from *B. subtilis* will have a different substrate profile and belong to another, closely related family of enzymes.

Pita Protects Glutamine Synthetase (GS). Deletion of pita activity caused *P. aeruginosa* to become very sensitive to growth inhibition by L-metsox on minimal media with all of the tested nitrogen sources except for L-glutamine. L-Glutamine is an essential intermediate in the pathway of nitrogen incorporation in bacteria (*44*) and is formed from L-glutamate, ATP, and ammonium by the activity of GS. L-Glutamate is formed from nitrogen sources either by the GS/glutamate synthase (GOGAT) pathway (e.g., from urea) or by the action of NADP-GDH (from ammonium) or directly (e.g., from proline) (*45*, *46*). L-Metsox, acting as an L-glutamate analogue, is a well-documented inhibitor of GS (*47*) so our observations indicate that growth inhibition of Depp4 by L-metsox is independent of the pathway of L-glutamate formation and is due to inhibition of GS activity. Support for this explanation was provided by L-metsox-resistant mutant strains, XN1 and XN4, derived from Depp4 that harbored mutations in GS. In both cases the mutations altered V214; this residue lies within a strongly conserved region of GS that constitutes part of the pocket in which the substrate L-glutamate and the inhibitors L-phosphinothricin and L-metsox bind (*28*). A detailed study of these mutated GSs is underway.

We conclude that the resistance of wild-type *P. aeruginosa* to the growth inhibitory effects of L-metsox is attributable to the pita-catalyzed acetylation of L-metsox preventing its inhibitory interaction with GS. L-Metsone, the other substrate of pita, is an inhibitor of glutamate synthase (*48*) and inhibits the growth of Depp4 on minimal medium in the absence of glutamate (Tata and Brown, unpublished results). Whether L-metsox and L-metsone are the natural substrates of pita is debatable; L-metsox is present in the bark and roots of plants belonging to the genus *Connaraceae* (*29*), but this limited occurrence seems unlikely to account for the widespread distribution of pita-like enzymes in bacteria. We cannot exclude the possibility that L-metsox or L-metsone or chemical derivatives could be intermediates in a biosynthetic pathway producing secondary metabolites with pita participating in a similar way to phosphinothricin acetyltransferase in the Bialaphos pathway. However, the *bar* gene encoding phosphinothricin acetyltransferase is in a cluster of genes encoding other enzymes of the Bialaphos pathway (*10*) whereas *pita* function appears to be unrelated to those of surrounding genes. Furthermore, we are unaware of any reports of the detection of L-metsone or of L-metsox in bacteria. Although L-methionine residues in proteins are susceptible to oxidation, the main product is methionine sulfoxide (*49*) that is not a pita substrate. The possibility remains that the naturally occurring substrate of pita is still to be found among the large number of compounds that are structurally related to L-metsox, and we are investigating several of these.

Sensitivity to L-metsox in the absence of pita, whether bacterial growth is nitrogen-limited (GS/GOGAT pathway) or not (NADP-GDH pathway), indicates that, normally, pita is synthesized under both growth conditions. An active uptake mechanism concentrating L-metsox is suggested by the difference between the K_m value of pita for L-metsox (1.3 mM) and the sensitivity of Depp4 to 5 μM L-metsox. Perhaps mutations affecting this uptake system account for the L-metsox resistance of strains XN2 and XN3, obtained from strain Depp4, that do not have alterations in GS. Since neither strain PAC1 nor Depp4 was sensitive to growth inhibition by phosphinothricin on minimal media, it seems likely that phosphinothricin is not taken up by *P. aeruginosa*.

Could Pita-like Enzymes Hinder the Development of Novel Antibiotics? GS, as an essential enzyme for growth in the absence of exogenous L-glutamine, is a potential antibiotic target. Inhibition by L-metsox of the secreted *Mycobacterium tuberculosis* GS encoded by the glnA1 gene protects guinea pigs against infection, leading to the proposal of L-metsox as a synergistic antibiotic with isoniazid against *M. tuberculosis* (*50*). *M. tuberculosis* does not have a pita homologue (based on the results of a BLAST search against the TB proteome) so the use of L-metsox as an antibiotic is not limited in that case. Our work suggests that the widespread distribution of pita homologues may restrict the use of L-metsox as a potential therapeutic agent to those organisms lacking such an enzyme, because of its protective role toward intracellular GS, unless an inhibitor could be designed. The structural data presented here provide a basis for the development of such an inhibitor.

ACKNOWLEDGMENT

We thank Michele Cianci, Mark Ellis, Rob Kehoe, Mike Macdonald, and James Nicholson for assistance during data collection at the SRS. Mary Holdom (King's College London) is also thanked for assistance during data collection.

REFERENCES

1. Davies, A. M., Tata, R., Agha, R., Sutton, B. J., and Brown, P. R. (2005) Crystal structure of a putative phosphinothricin acetyltransferase (PA4866) from *Pseudomonas aeruginosa* PAC1, *Proteins: Struct., Funct., Bioinf. 61*, 677−679.
2. Badger, J., Sauder, J. M., Adams, J. M., Antonysamy, S., Bain, K., Bergseid, M. G., Buchanan, S. G., Buchanan, M. D., Batiyenko, Y., Christopher, J. A., Emtage, S., Eroshkina, A., Feil, I., Furlong, E. B., Gajiwala, K. S., Gao, X., He, D., Hendle, J., Huber, A., Hoda, K., Kearins, P., Kissinger, C., Laubert, B., Lewis, H. A., Lin, J., Loomis, K., Lorimer, D., Louie, G., Maletic, M., Marsh, C. D., Miller, I., Molinari, J., Muller-Dieckmann, H. J., Newman, J. M., Noland, B. W., Pagarigan, B., Park, F., Peat, T. S., Post, K. W., Radojicic, S., Ramos, A., Romero, R., Rutter, M. E., Sanderson, W. E., Schwinn, K. D., Tresser, J., Winhoven, J., Wright, T. A., Wu, L., Xu, J., and Harris, T. J. (2005) Structural analysis of a set of proteins resulting from a bacterial genomics project, *Proteins: Struct., Funct., Bioinf. 60*, 787−796.
3. Mobley, H. L. T., Island, M. D., and Hausinger, R. P. (1995) Molecular biology of microbial ureases, *Microbiol. Rev. 59*, 451−480.
4. Stover, C. K., Pham, X. Q., Erwin, A. L., Mizoguchi, S. D., Warrener, P., Hickey, M. J., Brinkman, F. S. L., Hufnagle, W. O., Kowalik, D. J., Lagrou, M., Garber, R. L., Goltry, L., Tolentino, E., Westbrock-Wadman, S., Yuan, Y., Brody, L. L., Coulter, S. N., Folger, K. R., Kas, A., Larbig, K., Lim, R., Smith, K., Spencer, D., Wong, G. K.-S., Wu, Z., Paulsen, I. T., Reizer, J., Saier, M. H., Hancock, R. E. W., Lory, S., and Olson, M. V. (2000) Complete genome sequence of *Pseudomonas aeruginosa* PAO1, an opportunistic pathogen, *Nature 406*, 959−964.
5. Bateman, A., Coin, L., Durbin, R., Finn, R. O., Hollich, V., Griffiths-Jones, S., Khanna, A., Marshall, M., Moxon, S., Sonnhammer, E. L. L., Studholme, D. J., Yeats, C., and Eddy, S. R. (2004) The Pfam protein families database, *Nucleic Acids Res. 32*, D138−D141.
6. Thompson, J. D., Higgins, D. G., and Gibson, T. J. (1994) CLUSTAL W: improving the sensitivity of progressive multiple sequence alignment through sequence weighting, position-specific gap penalties and weight matrix choice, *Nucleic Acids Res. 22*, 4673−4680.
7. Hall, T. A. (1999) BioEdit: a user-friendly biological sequence alignment editor and analysis program for Windows 95/98/NT, *Nucleic Acids Symp. Ser. 41*, 95−98.
8. Wohlleben, W., Arnold, W., Broer, I., Hillemann, D., Strauch, E., and Puhler, A. (1988) Nucleotide sequence of the phosphinothricin N-acetyltransferase gene from *Streptomyces viridochromogenes* Tü494 and its expression in *Nicotiana tabacum*, *Gene 70*, 25−37.
9. Thompson, C. J., Movva, N. R., Tizard, R., Crameri, R., Davies, J. E., Lauwereys, M., and Botterman, J. (1987) Characterization of the herbicide-resistant gene bar from *Streptomyces hygroscopicus*, *EMBO J. 6*, 2519−2523.
10. Thompson, F. J., and Seto, H. (1995) Bialaphos, in *Genetics and Biochemistry of Antibiotic Production* (Vining, L. C., and Studdard, C., Eds.) pp 197−222, Butterworth Heinemann Bio/Technology, Oxford, U.K.
11. Shi, J., Ghirlando, R., Beavil, R. L., Beavil, A. J., Keown, M. B., Young, R. J., Owens, R. J., Sutton, B. J., and Gould, H. J. (1997) Interaction of the low-affinity receptor CD23/Fc epsilonRII lectin domain with the Fc epsilon3−4 fragment of human immunoglobulin E, *Biochemistry 36*, 2112−2122.
12. Ghirlando, R., Keown, M. B., MacKay, G. A., Lewis, M. S., Unkeless, J. C., and Gould, H. J. (1995) Stoichiometry and thermodynamics of the interaction between the Fc fragment of human IgG(1) and its low-affinity receptor Fc(gamma)RIII, *Biochemistry 34*, 13320−13327.
13. D'Halluin, K., De Block, M., Denecke, J., Janssens, J., Leemans, J., Reynaerts, A., and Botterman, J. (1992) The *bar* gene as selectable and screenable marker in plant engineering, *Methods Enzymol. 216*, 415−426.

14. Cornish-Bowden, A. (1995) *Fundamentals of Enzyme Kinetics*, Portland Press, Brookfield, VT.
15. Gasteiger, E., Hoogland, C., Gattiker, A., Duvaud, S., Wilkins, M. R., Appel, R. D., and Bairoch, A. (2005) Protein identification and analysis tools on the ExPASy server, in *The Proteomics Protocols Handbook* (Walker, J. M., Ed.) pp 571−607, Humana Press, Totowa, NJ.
16. Kelly, M., and Clarke, P. H. (1962) An inducible amidase produced by a strain of *Pseudomonas aeruginosa*, *J. Gen. Microbiol. 27*, 305−316.
17. Matos, J. A. S. P. (2002) Studies on the urease operon of *Pseudomonas aeruginosa*, Ph.D. Thesis, University of London.
18. Brammar, W. J., and Clarke, P. H. (1964) Induction and repression of *Pseudomonas aeruginosa* amidases, *J. Gen. Microbiol. 37*, 307−319.
19. Wong, S., and Mekalanos, J. J. (2000) Genetic footprinting with mariner-base transposition in *Pseudomonas aeruginosa*, *Proc. Natl. Acad. Sci. U.S.A. 97*, 10191−10196.
20. Schweizer, H. P., and Hoang, T. T. (1995) An improved system for gene replacement and xylE fusion analysis in *Pseudomonas aeruginosa*, *Gene 158*, 15−22.
21. Cianci, M., Antonyuk, S., Bliss, N., Bailey, M. W., Buffey, S. G., Cheung, K. C., Clarke, J. A., Derbyshire, G. E., Ellis, M. J., Enderby, M. J., Grant, A. F., Holbourn, M. P., Laundy, D., Nave, C., Ryder, R., Stephenson, P., Helliwell, J. R., and Hasnain, S. S. (2005) A high-throughput structural biology/proteomics beamline at the SRS on a new multipole wiggler, *J. Synchrotron Radiat. 12*, 455−466.
22. Otwinowski, Z., and Minor, W. (1997) Processing of X-ray diffraction data collected in oscillation mode, *Methods Enzymol. 276*, 307−325.
23. Leslie, A. G. E. (1992) Recent changes to the MOSFLM package for processing film and image plate data, Joint CCP4 + ESF-EAMCB Newsletter on Protein Crystallography, No. 26.
24. CCP4, Collaborative Computational Project, Number 4 (1994) The CCP4 suite: programs for protein crystallography, *Acta Crystallogr. D50*, 760−763.
25. Vagin, A., and Teplyakov, A. (1997) MOLREP: an automated program for molecular replacement, *J. Appl. Crystallogr. 30*, 1022−1025.
26. Brünger, A. T., Adams, P. D., Clore, G. M., DeLano, W. L., Gros, P., Grosse-Kunstleve, R. W., Jiang, J., Kuszewski, J., Nilges, M., Pannu, N. S., Read, R. J., Rice, L. M., Simonson, T., and Warren, G. L. (1998) Crystallography & NMR system: a new software suite for macromolecular structure determination, *Acta Crystallogr. D54*, 905−921.
27. Molecular Simulation Inc. (2000) QUANTA2000, San Diego, CA.
28. Gill, H. S., and Eisenberg, D. (2001) The crystal structure of phosphinothricin in the active site of glutamine synthetase illuminates the mechanism of enzymatic inhibition, *Biochemistry 40*, 1903−1912.
29. Chevrier, B., Moras, D., Jeannoda, V. L. R., Creppy, E. E., and Dirheimer, G. (1986) Absolute configuration of natural methionine sulfoximine, *Acta Crystallogr. C42*, 1632−1634.
30. Schuettelkopf, A. W., and van Aalten, D. M. F. (2004) PRODRG—a tool for high-throughput crystallography of protein-ligand complexes, *Acta Crystallogr. D60*, 1355−1363.
31. Kleywegt, G. J., and Jones, T. A. (1998) Databases in protein crystallography, *Acta Crystallogr. D54*, 1119−1131.
32. Laskowski, R. A., MacArthur, M. W., Moss, D. S., and Thornton, J. M. (1993) PROCHECK—a program to check the stereochemical quality of protein structures, *J. Appl. Crystallogr. 26*, 283−291.
33. Vaguine, A. A., Richelle, J., and Wodak, S. J. (1999) SFCHECK: a unified set of procedures for evaluating the quality of macromolecular structure-factor data and their agreement with the atomic model, *Acta Crystallogr. D55*, 191−205.
34. Emsley, P., and Cowtan, K. (2004) Coot: model-building tools for molecular graphics, *Acta Crystallogr. D60*, 2126−2132.
35. Kabsch, W., and Sander, C. (1983) Dictionary of protein secondary structure: pattern recognition of hydrogen-bonded and geometrical features, *Biopolymers 22*, 2577−2637.
36. Holm, L., and Sander, C. (1994) The FSSP database of structurally aligned protein fold families, *Nucleic Acids Res. 22*, 3600−3609.
37. Berman, H. M., Westbrook, J., Feng, Z., Gilliland, G., Bhat, T. N., Weissig, H., Shindvalov, I. N., and Bourne, P. E. (2000) The Protein Data Bank, *Nucleic Acids Res. 28*, 235−242.
38. Neuwald, A. F., and Landsman, D. (1997) GCN5-related histone N-acetyltransferases belong to a diverse superfamily that includes the yeast SPT10 protein, *Trends Biochem. Sci. 22*, 154−155.
39. DeLano, W. L. (2002) The PyMOL molecular graphics system, DeLano Scientific, San Carlos, CA.
40. Peneff, C., Mengin-Lecreulx, D., and Bourne, Y. (2001) The crystal structures of apo and complexed *Saccharomyces cerevisiae* GNA1 shed light on the catalytic mechanism of an amino-sugar N-acetyltransferase, *J. Biol. Chem. 276*, 16328−16334.
41. Burk, D. L., Ghuman, N., Wybenga-Groot, L. E., and Berghuis, A. M. (2003) X-ray structure of the AAC(6′)-Ii antibiotic resistance enzyme at 1.8Å resolution; examination of oligomeric arrangements in GNAT superfamily members, *Protein Sci. 12*, 426−437.
42. Vetting, M. W., de Carvalho, L. P. S., Roderick, S. L., and Blanchard, J. S. (2005) A novel dimeric structure of the RimL N^{α}-acetyltransferase from *Salmonella typhimurium*, *J. Biol. Chem. 280*, 22108−22114.
43. He, H., Ding, Y., Bartlam, M., Sun, F., Le, Y., Qin, X., Tang, H., Zhang, R., Joachimiak, A., Liu, Y., Zhao, N., and Rao, A. (2003) Crystal structure of tabtoxin resistance protein complexed with acetyl coenzyme A reveals the mechanism for β-lactam acetylation, *J. Mol. Biol. 325*, 1019−1030.
44. Merrick, M. J., and Edwards, R. A. (1995) Nitrogen control in bacteria, *Microbiol. Rev. 59*, 604−622.
45. Brown, P. R., and Tata, R. (1981) Growth of *Pseudomonas aeruginosa* mutants lacking glutamate synthase activity, *J. Bacteriol. 147*, 193−197.
46. Hashim, S., Kwon, D. H., Abdelal, A., and Lu, C. D. (2004) The arginine regulatory protein mediates repression by arginine of the operons encoding glutamate synthase and anabolic glutamate dehydrogenase in *Pseudomonas aeruginosa*, *J. Bacteriol. 186*, 3848−3854.
47. Meister, A. (1980) in *Glutamine: Metabolism, Enzymology, and Regulation* (Mora, J., and Palacios, R., Eds.) pp 1−59, Academic Press, New York.
48. Masters, D. S., and Meister, A. (1982) Inhibition by homocysteine sulphonamide of glutamate synthase purified from *Saccharomyces cerevisiae*, *J. Biol. Chem. 257*, 8711−8715.
49. Jacob, C., Giles, G. I., Giles, N. M., and Sies, H. (2003) Sulfur and selenium: the role of oxidation state in protein structure and function, *Angew. Chem., Int. Ed. 42*, 4742−4758.
50. Harth, G., and Horwitz, M. A. (2003) Inhibition of *Mycobacterium tuberculosis* glutamine synthetase as a novel antibiotic strategy against tuberculosis: demonstration of efficacy in vivo, *Infect. Immun. 71*, 456−464.

BI0615238